Magnetic suspension performance enhancement of ultra-compact 5-DOF controlled self-bearing motor for rotary pediatric ventricular assist device

Masahiro Osa [a], Toru Masuzawa [a], Ryoga Orihara [a] , Eisuke Tatsumi [b]

[a] Ibaraki University, 4-12-1 Nakanarusawa, Hitachi, Japan, Masahiro.osa.630@vc.ibaraki.ac.jp
[b] National cerebral and cardiovascular center research institute, 5-7-1 Fujishirodai, Suita, Japan

***Abstract*— Research interests of the compact magnetically levitated motor have been strongly increased in development of durable and biocompatible mechanical circulatory support (MCS) devices for pediatric heart disease patients. In this study, a tiny axial gap type 5-degrees of freedom (DOF) controlled self-bearing motor for use in pediatric MCS devices has been developed. The motor consists of two identical motor stators and a centrifugal levitated rotor. This paper investigated design improvement of the magnetic circuit for the developing self-bearing motor to enhance the magnetic suspension and rotation performance. The motor geometries were refined by using numerical calculation and three-dimensional magnetic field analysis. The modified motor can achieve the higher suspension force and torque characteristics than the previously developed motor, and indicates stable magnetic suspension performance up to the rotating speed of 8000 rpm.**

I. INTRODUCTION

Mechanical circulatory support (MCS) is widely used for heart disease therapy. Currently, there have been increasing research interests in pediatric heart treatment with MCS devices [1]. A significantly tiny rotary MCS device for pediatric circulation is being developed by Jarvik Heart Inc in US [2-3]. However, the Jarvik device is now facing technical difficulties such as deterioration of mechanical durability, blood clotting and blood destruction, due to a mechanically contacting bearing to suspend a spinning rotor impeller. Hence, development of next generation MCS device which can completely levitate a rotating impeller is strongly demanded due to high durability and better blood compatibility.

Magnetic suspension system is one of a candidate to suspend the rotating impeller without mechanical contact. Reduction of actively controlled positions is general strategy to miniaturize the magnetic suspension systems [4-7]. For example, 2-digrees of freedom (-DOF) controlled radial maglev motors and 3-DOF controlled double stator axial maglev motors have been developed [8-11]. These miniaturized maglev motors are successfully applied to implantable and extracorporeal MCS devices for adult patients, whereas further miniaturization of the maglev motors is required for use in rotary pediatric MCS devices.

This study has been developing a compact pediatric MCS device with 5-DOF controlled self-bearing motor, and the developed device demonstrated noncontact suspension and a sufficient pump performance [12-14]. However, further improvement of magnetic suspension stability is necessary to achieve higher mechanical reliability and energy conservation system required for clinically applicable MCS devices. In this paper, design improvement of magnetic circuit for the 5-DOF controlled self-bearing motor was investigated to enhance the magnetic suspension performance and energy efficiency by using theoretically calculation and three-dimensional (3D) finite element method (FEM) analysis. In addition, static force and torque characteristics, dynamic magnetic suspension performance and energy consumption of the improved maglev motor are evaluated.

II. 5-DOF CONTROLLED SELF-BEARING MOTOR FOR PEDIATRIC VENTRICULAR ASSIST DEVICE

A. Over view of maglev pediatric VAD with 5-DOF controlled self-bearing motor

The 5-DOF controlled self-bearing motor is driven as an axial gap type surface permanent magnet synchronous motor which has 6-slot and 4-pole structure. Fig. 1 shows a schematic of the self-bearing motor which is consists of two identical motor stators and a levitated impeller. The levitated impeller is axially suspended with the both stators. Integrated windings for suspension and rotation control are wound on each stator tooth. A motor torque and a suspension force are produced with double stator mechanism. An axial position (z) and rotating speed (ωz) are actively regulated with a 4-pole control magnetic field. Radial positions (x and y) and tilting angles (θx and θx) are actively regulated with a 2-pole control magnetic field. 5-DOF of impeller postures are independently regulated by overlapping the different control magnetic fields in the air-gap [1].

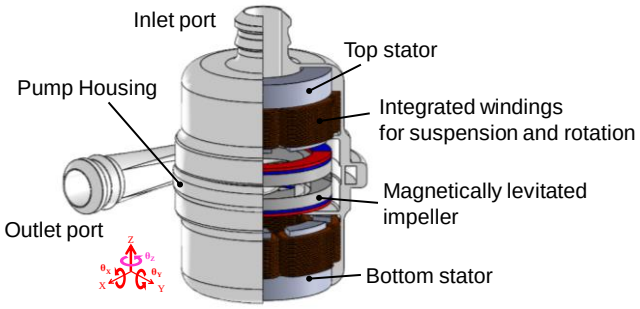

Figure 1. Stracture of pedatric ventricular assist device with the axial gap type double stator 5-DOF controlled self-bearing motor.

B. *Characteristics of suspension force and torque*

The motor produces axial suspension force and rotating torque with a single rotating magnetic field based on vector control algorithm. An axial position (z) of the levitated impeller is actively regulated by field strengthening and field weakening as shown in Fig. 2. A rotating speed (ω_z) of the rotor is controlled by conventional q-axis current regulation. The axial suspension force and the rotating torque are linearly produced with d-axis current i_d and q-axis current i_q.

$$F_z = k_{Fz}(i_d - i'_d) \quad (1)$$

$$T_{\theta z} = k_{T\theta z}(i_q + i'_q) \quad (2)$$

Inclination angles (θ_x and θ_y) and radial positions (x and y) of the levitated rotor can be controlled with p$\pm$2 pole algorithm. The control magnetic field can simultaneously produce an inclination torque and a radial suspension force. Inclination torque around y-axis and the radial suspension force in x direction are produced with the double stator mechanism as shown in Fig. 3. The magnitude and the direction of the inclination torque and the radial suspension force can be linearly regulated with respect to excitation current supplied to the top stator and the bottom stator as following equations.

$$T_{\theta x/y} = k_{T\theta x/y}(i_{top} + i_{bottom}) \quad (3)$$

$$F_{x/y} = k_{Fx/y}(i_{top} - i_{bottom}) \quad (4)$$

III. SUSPENSION FORCE AND TORQUE ENHANCEMENT WITH MODIFIED MAGNETIC CIRCUIT OF THE MAGLEV MOTOR

A. *Design strategy of suspension performance enhancement*

The motor uses flux density produced by the permanent magnet as a main flux density to produce the suspension force and the rotating torque. Enhancement of the permanent magnet flux contributes to higher suspension force production. However, in miniaturized motor, there is difficulty to have sufficiently large cross-sectional area of the magnetic flux path, and it has possibility of deterioration of magnetic suspension force due to the magnetic saturation. Furthermore, excessively increased negative stiffness due to the high magnetic intensity potentially deteriorate controllability of the magnetic system. Hence, well design of the magnetic circuit which can keep a good balance between magnetic flux density produced by the permanent magnet and electromagnet is required to achieve sufficient magnetic suspension stability. In this study, design goal is to enhance the suspension force produced by the electromagnet without change of non-excited axial attractive force for avoiding instability caused due to the axial negative stiffness.

B. *Design refinment of magnetic circuit for 5-DOF controlled self-bearing motor to enhance the suspension force and torque*

Design improvement of a magnetic circuit for the 5-DOF controlled self-bearing motor was performed based on following design strategy to enhance the magnetic suspension performance. 1) Keeping device size such as the outer diameter, the total height and the total volume of the previously developed prototype motor. 2) Maintaining the axial negative stiffness kz within +/-10% of that produced by the previously developed prototype motor. 3) Maximizing the force coefficient in the axial direction ki defined as a slope of the suspension force to excitation current.

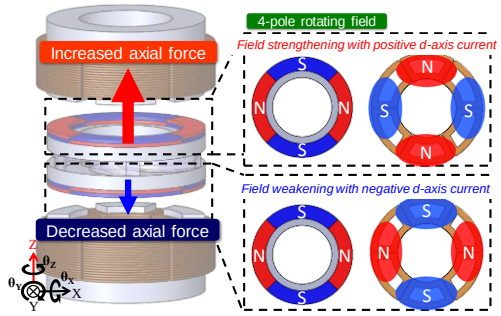

Figure 2. Axial position control by utilizing field strengthening and field weakening.

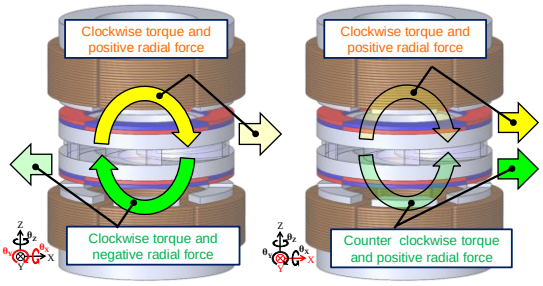

Figure 3. Inclination and radial position control with p +/-2 pole rotating magnetic field.

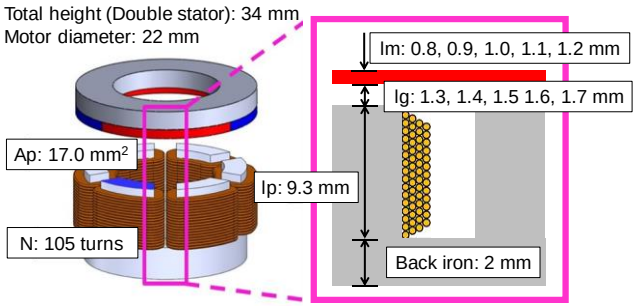

Figure 4. Variable geometries of magnetic circuit for the self-bearing motor in design improvement using 3-D FEM magnetic field simulation.

Geometries representatively characterizing the magnetic circuit of the self-bearing motor: pole height lp, pole cross sectional area Ap, air-gap length lg and permanent magnet thickness lm, were numerically designed with theoretical calculation and fixed by using 3-D FEM magnetic field analysis as shown in Fig.2. Height and cross-sectional area of the stator pole were determined as 9.3 mm and 17.0 mm^2 in order to effectively maximize the force coefficient with slight change of the negative stiffness and the non-excited force. Parametric study in the air-gap length and the PM thickness were performed. Variable parameters of the air-gap length of 1.3-1.7 mm and the PM thickness of 0.8-1.2 mm were chosen to be available to fabrication. Each combination of the air-gap length and PM thickness were simulated, and the non-excited axial negative stiffness kz and the force coefficient ki were estimated.

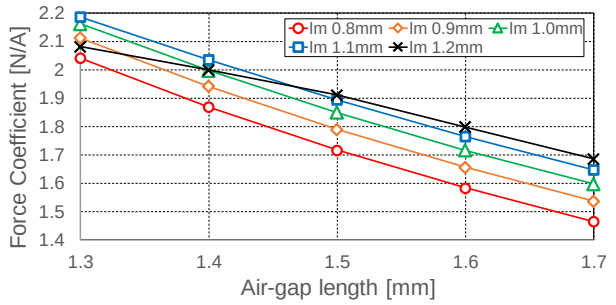

(a) Force coefficient

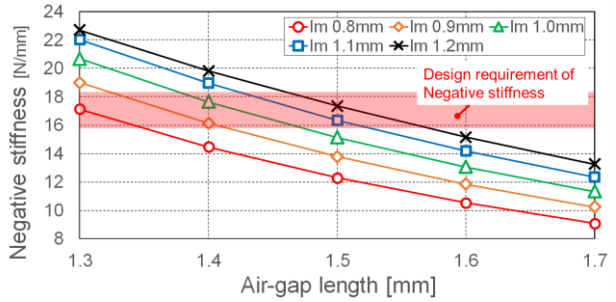

(b) Axial negative stiffnesse

Figure 5. Estimated force coefficient and non-excited axial force Fz and at different air-gap length and PM thickness.

The numerically estimated force coefficient and non-excited attractive force of the self-bearing motor with different geometries in the air-gap length and the PM thickness are shown in Fig.5. The optimal geometries in FEM simulation to maximize the force coefficient (ki < 1.2 N/A) and maintain the axial negative stiffness (15.2 N/mm < kz < 18.6 N/mm) are the shortest air-gap length of 1.3 mm and the thinnest PM excited force of the optimally designed motor are 2.0 N/A and 6.1 N. Deterioration of the magnetic flux density with reduction of the PM thickness can be compensated by reducing the air-gap length. The shorter air-gap length and the thinner PM thickness can reduce magnetic resistance for the electromagnet and effectively enhance the magnetic suspension force production with excitation current.

IV. Developed System of 5-DOF Controlled Maglev Motor with Modified Magnetic Circuit

A. *Fabrication of 5-DOF controlled maglev motor*

A 5-DOF controlled self-bearing motor for pediatric VAD shown in Fig. 6 was developed referring to motor geometries determined by using 3D FEM magnetic field analysis. the outer diameter and total height are 22 mm and 33 mm. The length of magnetic air-gap of the developed motor is set to 1.3 mm. The material used for magnetic core of the motor stator and the rotor back iron is soft magnetic iron (SUY-1). The permanent magnets of 0.8 mm thickness are made of Nd- Fe-B, that has coercivity and residual flux density of 907 kA/m and 1.36 T, respectively. Concentrated cupper windings of 105 turns are wound on each stator tooth. Pump clearance between the pump casing and levitated rotor in the axial and radial direction are 0.3 mm and 0.5 mm.

B. *Control system for magnetic levitation and rotation with digital PID controllers*

Digital PID controllers are implemented on a micro

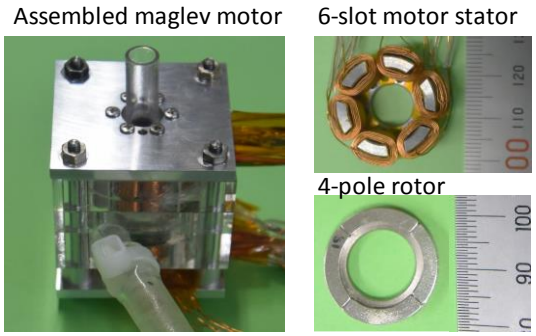

Figure 6. Developed 5-DOF controlled maglev motor with modified magnetic circuit.

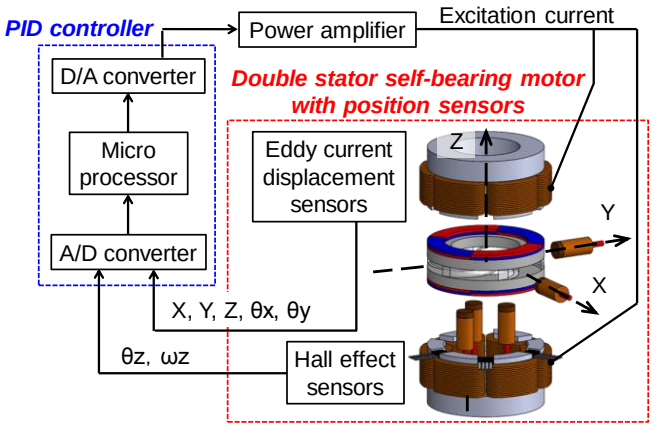

Figure 7. Schematic diagram of 5-DOF controlled maglev motor.

processor board DS1104 (dSPACE GmbH, Paderborn Germany) with MATLAB/Simlink for 5-DOF active control. Fig. 7 shows a schematic diagram of a 5-DOF control system. An axial position and inclination angles around x and y axes of the levitated rotor are measured by three eddy current sensors (PU-03A, Applied Electronics Corporation). Radial positions of the levitated rotor in x and y direction are measured with other two eddy current sensors. A rotating angle of the levitated rotor is determined by outputs of three Hall Effect sensors (Asahi KASEI Corporation) with a sensitivity of 30 degrees electrical angle. The rotating speed is calculated by time derivative of the rotating angle. Required control current is calculated with PID controllers and is supplied by power amplifier (PA12A, Apex Microtechnology Corporation) to the both stators windings. Sampling and control frequency is 10 kHz. Control gains of digital PID controllers for magnetic suspension and rotation were determined based on the previously measured motor suspension force and torque characteristics, and then, manually tuned in dynamic performance evaluation.

A block diagram for axial position and rotation control, inclination angle and radial position control are shown in Fig. 8 and Fig. 9, respectively. Positive and negative d-axis current are determined by a PID feedback loop to produce an axial suspension force. q-axis current of both stators is regulated with a PI feedback loop for a conventional rotating speed control. Required current for inclination angle and radial position control are calculated by other four PID feedback loops to determine amplitude and phase angle of two-pole rotating magnetic field produce by the top and bottom stators.

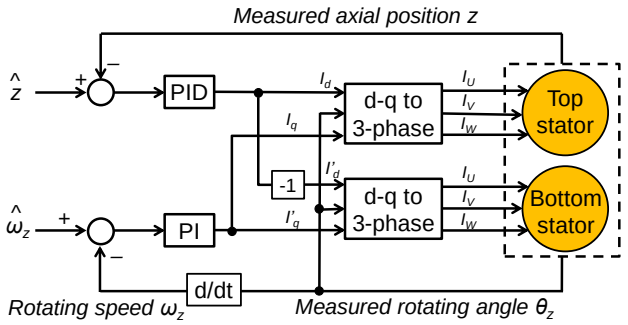

Figure 8. Block diagram of feedback loop for the axial position and the rotating speed regulation.

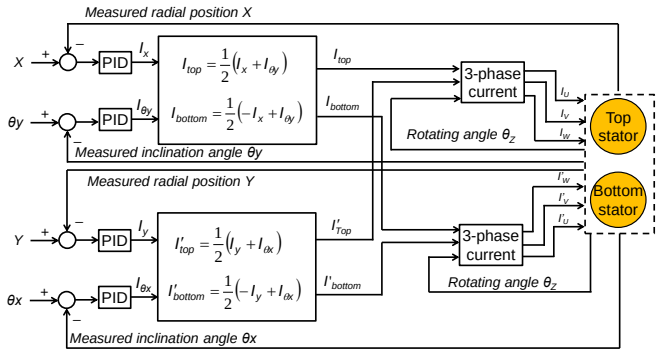

Figure 9. Block diagram of feedback loop for the inclination and the radial .

V. MAGNETIC SUSPENSION PERFORMANCE EVALUATION OF DEVELOPED MAGLEV MOTOR

A. *Static magnetic suspension performance measurement*

Static magnetic suspension force and torque characteristics: an axial negative stiffness kz, a radial stiffness kr, and suspension force of the designed motor was evaluated. The axial and radial suspension force and the inclination torque were produced at excitation current of 1 A and air-gap length of 1.3 mm.

B. *Dynamic characteristics of developed 5-DOF controlled maglev motor*

The rotor was magnetically levitated in water medium with 3-DOF control as an initial step. 3-DOF control was chosen to evaluate basic characteristics of stabilization in unstable axes: axial direction and inclination around x and y axes. The radial position of the rotor is passively stabilized in this paper. Magnetic suspension performance with respect to increase in the rotating speed of the rotor was evaluated. The rotating speed was increased from 1000 rpm to 8000 rpm. Oscillation amplitude in axial direction and radial direction, maximum inclination angle around x and y axes, and power consumption of the motor during magnetic levitation and rotation were evaluated. The maximum oscillation amplitude was defined as half of the peak-to-peak value of rotor vibration.

VI. RESULTS

Static suspension characteristics: stiffness, suspension force and torque, of the developed maglev motor which has the modified magnetic circuit and the previously developed maglev motor are shown together in Fig.11. The Axial

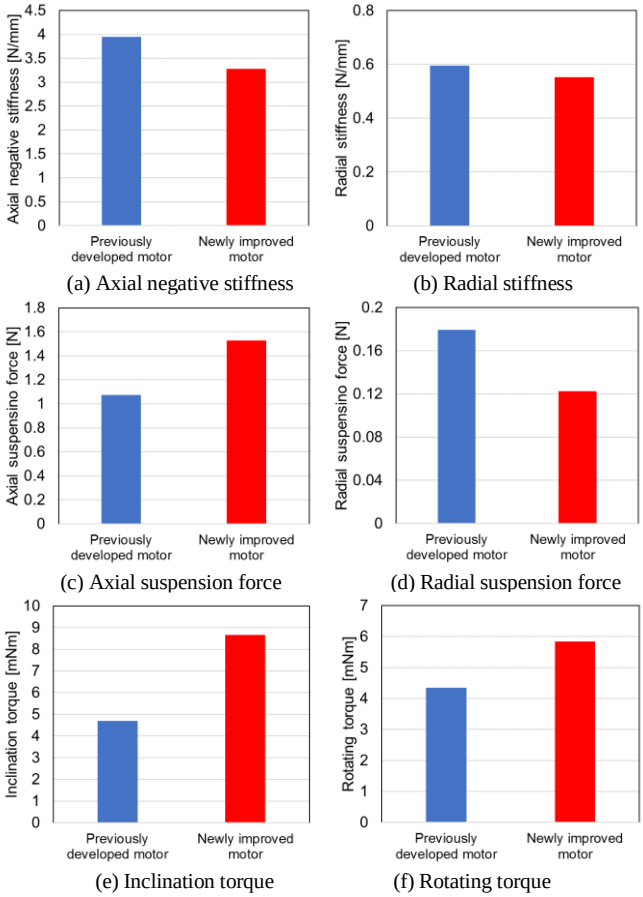

Figure 10. Static suspension characteristeics of the developed maglev motor. (a), (b): Axial and radial stiffness. (c), (d): Magnetic suspension force in axial and radial direction at excitation current of 1 A. (e), (f): Torque characteristics at excitation current of 1A.

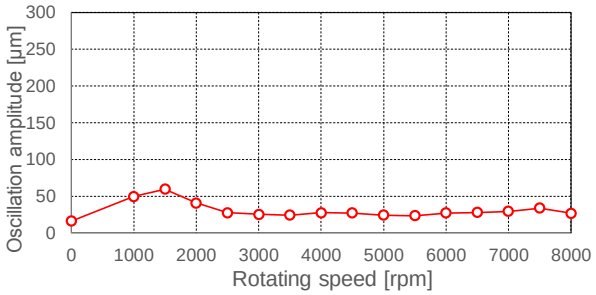

Figure 11. Maximum oscillation apmlitude of the levitated and rotated rotor in axial direction.

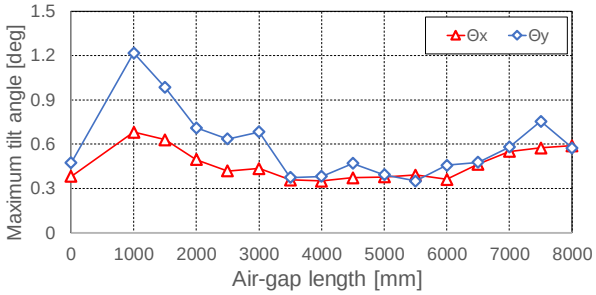

Figure 12. Maximum inclination angle of the levitated and rotated rotor around x and y axes..

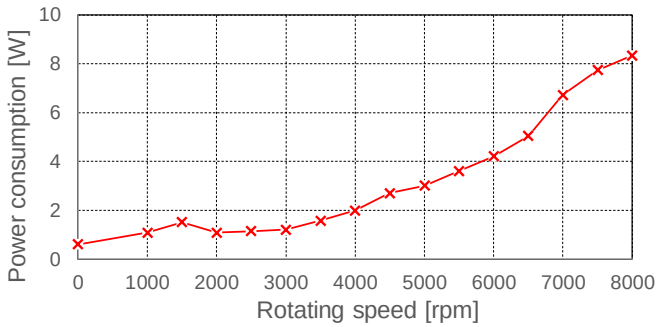

Figure 13. Power consumption of the developed maglev motor with respect to the increase in the rotating speed.

negative stiffness of the improved motor decreased to 1N, however, the radial stiffness was not significant change. The deterioration of the radial passive stability did not occur. The axial suspension force increased to 1N, and the radial suspension force slightly decreased. Both the inclination torque and the rotating torque increased to 1mNm and 1 mNm, respectively.

The improved motor successfully achieves non-contact levitation and rotation up to the rotating speed of 8000 rpm. The maximum axial oscillation amplitude and the maximum inclination angle around x and y axes with respect to the increase in the rotating speed of the levitated rotor are shown in Fig. 12. In the lower speed range from 1000-3000 rpm, the oscillation of the levitated rotor was slightly increased. In contrast, the oscillation amplitude and the inclination angle were significantly suppressed around 30 μm and 0.3 deg at the operational pump speeds of 4000-6000 rpm by enhancement of the suspension characteristics. The power consumption of the developed motor during magnetic levitation and rotation was in the range of 2-8 W at the rotating speeds of 1000-8000 rpm.

V. Discussion

Impeller suspension technique using magnetic suspension much contributes to enhance device durability and blood compatibility of the rotary MCS devices. In ultra-compact maglev motor, optimization of the magnetic circuit for suspension system plays a significant role in the next generation rotary pediatric VADs development.

The developed maglev motor successfully achieves the much higher suspension force coefficient ki maintaining the negative stiffness kz in the axial suspension characteristics. a suspension index defined as ki/kz=1 is significantly higher than that of the previously developed motor (ki/kz=1). Although the radial suspension characteristics slightly decreased, the deterioration of the total magnetic suspension performance will not occur because the magnitude of the radial suspension force is absolutely small. Even the radial suspension force produced by the newly developed motor is much effective to suppress the resonance and disturbance. The grossly increased inclination torque and the rotating torque will contribute to achieve better suspension stability and low energy consumption.

The axial oscillation amplitude and the inclination angle were well suppressed, and resonance peak was not found at any rotating speed. Detail evaluation changing the rotating speed precisely should be required to investigate advanced dynamic characteristics. Suspension performance evaluation with radial position control will also be required to characterize the total system of the developed 5-DOF controlled maglev motor. However, it can be seen from the experimental results that the resonance frequency calculated from the mass and the system stiffness must be lower than operational frequency of the pediatric pump, it does not influence actual pump operation.

The power consumption at the operating speed range of the pediatric VAD was 2-4 W. The improved motor with modified magnetic circuit achieved more than 50% reduction of the power consumption compare with that of the previously developed motor. The input power increased as increase in the rotating speed. This is due to increase in the suspension current at higher speed rotation and the iron loss. Material change of the stator magnetic core will effectively reduce power consumption at higher rotating speed.

VI. Conclusion

The ultra-compact 5-DOF controlled self-bearing motor has been developed for pediatric MCS devices. The static magnetic suspension characteristics were successfully improved by refining the magnetic circuit of the motor. The dynamic magnetic suspension performance and energy efficiency is also improved, and further stable magnetic suspension with high speed rotation is successfully indicated. As a next step, evaluation of radial suspension performance will be performed and then pump performance of pediatric rotary VAD will be investigated.

Acknowledgment

This work was supported by Japanese Society for the Promotion of Science (JSPS) KAKENHI Grant-in-Aid for Young Scientists (B) Grant Number 16K18036.

References

[1] J.Timothy Baldwin, Harvey S. Borovets, Brian W. Duncan, Mark J. Gartner, Robert K. Jarvik, William J. Weiss and Tracey R. Hoke, The National Heart, Lung, and Blood Institute Pediatric Circulatory Support, Journal of the American heart association, pp. 147-155, 2006.

[2] Marc Gibber, Zhongjun J. Wu, Won-Bae Chang, Giacomo Bianchi, Jingping Hu, Jose Garcia, Robert Jarvik, Bartley P. Griffith, In Vivo Experience of the Child-Size Pediatric Jarvik 2000 Heart: Update, ASAIO Journal, Vol. 56, No. 4, 2010.

[3] X. Wei, T. Li, S. Li, J. Sung, P. Sanchez, S. Niu, C. Watkins, C. DeFilippi, R. Jarvik, Z. J. Wu, B. P. Griffith, Pre-clinical evaluation of the infant Jarvik 2000 heart in a neonate piglet model, The Journal of Heart and Lung Transplantation, Vol. 32, No. 1, pp. 112-119, 2013.

[4] A. Yukawa, T. Shinshi, X.Zhang, H. Tachikawa and A.Shimokohbe, A One-DOF Controlled Magnetic Bearing for Compact Centrifugal Blood Pumps, Motion and Vibration Control, Springer Science+Business Media B.V., pp. 357-366, 2009.

[5] Quang Dich Nguyen, Satoshi Ueno, Analysis and Control of Nonsalient Permanent Magnet Axial Gap Self-Bearing Motor, IEEE Transactions on Industrial Electronics, Vol. 58, No. 7, pp. 2644-2652, 2011.

[6] Junichi Asama, Yuki Hamasaki, Takaaki Oiwa, Akira Chiba, Proposal and Analysis of a Novel Single-Drive Bearingless Motor, IEEE Transactions on Industrial Electronics, Vol. 60, No. 1, pp. 129-138, 2013.

[7] R. Takeda, S. Ueno, C. Jiang, Development of a Centrifugal Cryogenic Fluid Pump using an Axial Self-bearing Motor, Proceedings of ISMB15, pp. 693-700, 2016.
[8] Daniel L. Timms, Nobuyuki Kurita, Nicholas Greatrex, Toru Masuzawa, BiVACOR A Magnetically Levitated Biventricualr Artificial Heart, Proc. of MAGDA conference in Pacific Asia, pp.482-487, 2011.
[9] M Osa, T. Masuzawa, E. Tatsumi, Miniaturized axial gap maglev motor with vector control for pediatric artificial heart, Journal of JSAEM, Vol.20, No. 2, pp. 397-403, 2012.
[10] N. Kurita, T. Ishikawa, N. Saito, T. Masuzawa, Basic Design of the Maglev Pump for Total Artificial Heart by using Double Stator Type Axial Self-bearing Motor, Proceedings of ISMB15, pp. 509-514, 2016.
[11] Mandeep R. Mehra, Yoshifumi Naka, Nir Uriel, et al, A Fully Magnetically Levitated Circulatory Pump for Advanced Heart Failure, The NEW ENGLAND JOURNAL of MEDICINE, pp. 1-11, 2016.
[12] M Osa, T. Masuzawa, Tatsumi, 5-DOF control double stator motor for paediatric ventricular assist device, Proceedings of ISMB13, pp. paper 41 (9 pages), 2012.
[13] M Osa, T. Masuzawa, N. Omori, E. Tatsumi, Radial position active control of double stator axial gap self-bearing motor for pediatric VAD, JSME Journal, Vol.2, No. 4, pp. 1-12, 2015.
[14] M Osa, T. Masuzawa, T. Saito., E. Tatsumi, Miniaturizing 5-DOF fully controlled axial gap maglev motor for pediatric ventricular assist devices, International Journal of AEM, Vol.52, No. 1-2, pp. 191-198, 2016.